Quaternary Science Reviews 75 (2013) 181–194

Contents lists available at SciVerse ScienceDirect

Quaternary Science Reviews

journal homepage: www.elsevier.com/locate/quascirev

An alternative suggestion for the Pliocene onset of major northern hemisphere glaciation based on the geochemical provenance of North Atlantic Ocean ice-rafted debris

Ian Bailey[a,*], Georgia M. Hole[a,b], Gavin L. Foster[a], Paul A. Wilson[a], Craig D. Storey[c], Clive N. Trueman[a], Maureen E. Raymo[d]

[a] National Oceanography Centre Southampton, University of Southampton, Waterfront Campus, European Way, Southampton SO14 3ZH, UK
[b] Department of Earth Science and Engineering, Imperial College, London SW7 2AZ, UK
[c] School of Earth & Environmental Sciences, Burnaby Building, Burnaby Road, Portsmouth PO1 3QL, UK
[d] Columbia University, Lamont-Doherty Earth Observatory, P.O. Box 1000, 61 Route 9W, Palisades, NY 10964, USA

ARTICLE INFO

Article history:
Received 20 February 2013
Received in revised form
27 May 2013
Accepted 10 June 2013
Available online 16 July 2013

Keywords:
Provenance
Ice-rafted debris
Lead isotopes
Laser ablation
Northern hemisphere glaciation
Pliocene
Quaternary

ABSTRACT

The onset of abundant ice-rafted debris (IRD) deposition in the Nordic Seas and subpolar North Atlantic Ocean 2.72 millions of years ago (Ma) is thought to record the Pliocene onset of major northern hemisphere glaciation (NHG) due to a synchronous advance of North American Laurentide, Scandinavian and Greenland ice-sheets to their marine calving margins during marine isotope stage (MIS) G6. Numerous marine and terrestrial records from the Nordic Seas region indicate that extensive ice sheets on Greenland and Scandinavia increased IRD inputs to these seas from 2.72 Ma. The timing of ice-sheet expansion on North America as tracked by IRD deposition in the subpolar North Atlantic Ocean, however, is less clear because both Europe and North America are potential sources for icebergs in this region. Moreover, cosmogenic-dating of terrestrial tills on North America indicate that the Laurentide Ice Sheet did not extend to ~39°N until 2.4 ± 0.14 Ma, at least 180 ka after the onset of major IRD deposition at 2.72 Ma. To address this problem, we present the first detailed analysis of the geochemical provenance of individual sand-sized IRD deposited in the subpolar North Atlantic Ocean between MIS G6 and 100 (~2.72–2.52 Ma). IRD provenance is assessed using laser ablation lead (Pb) isotope analyses of single ice-rafted (>150 μm) feldspar grains. To track when an ice-rafting setting consistent with major NHG first occurred in the North Atlantic Ocean during the Pliocene intensification of NHG (iNHG), we investigate when the Pb-isotope composition ($^{206}Pb/^{204}Pb$, $^{207}Pb/^{204}Pb$, $^{208}Pb/^{204}Pb$) of feldspars deposited at DSDP Site 611 first resembles that determined for IRD deposited at this site during MIS 100 (2.52 Ma), the oldest glacial for which there exists convincing evidence for widespread glaciation of North America. Whilst Quaternary-magnitude IRD fluxes exist at Site 611 during glacials from 2.72 Ma, we find that the provenance of this IRD is not constant. Instead, we find that the Pb-isotope composition of IRD at our study site is not consistent with major NHG until MIS G2 (2.64 Ma). We hypothesise that IRD deposition in the North Atlantic Ocean prior to MIS G2 was dominated by iceberg calving from Greenland and Scandinavia. We further suggest that the grounding line of continental ice on Northeast America may not have extended onto the continental shelf and calved significant numbers of icebergs to the North Atlantic Ocean during glacials until 2.64 Ma.

1. Introduction

The secular onset of widespread deposition of abundant ice-rafted debris (IRD) in the Nordic Seas and subpolar North Atlantic Ocean (Fig. 1) at 2.72 Ma (during marine isotope stage, MIS, G6, Fig. 2; Maslin et al., 1998; Kleiven et al., 2002) provides irrefutable evidence that a long-term increase in the oxygen isotope composition ($\delta^{18}O$) of benthic foraminifera over 3.5–2.5 Ma (Mudelsee and Raymo, 2005) documents a Plio–Pleistocene intensification of northern hemisphere glaciation (iNHG). The relative contributions of ice-sheet expansion on Greenland, Scandinavia and North America to the increases in $\delta^{18}O$ and IRD at this time, however, remain poorly constrained.

On the basis of pioneering research on cores recovered by the Deep Sea Drilling Project (DSDP) and Ocean Drilling Program (ODP)

* Corresponding author.
E-mail address: Ian.Bailey@noc.soton.ac.uk (I. Bailey).

0277-3791/$ – see front matter © 2013 Elsevier Ltd. All rights reserved.
http://dx.doi.org/10.1016/j.quascirev.2013.06.004

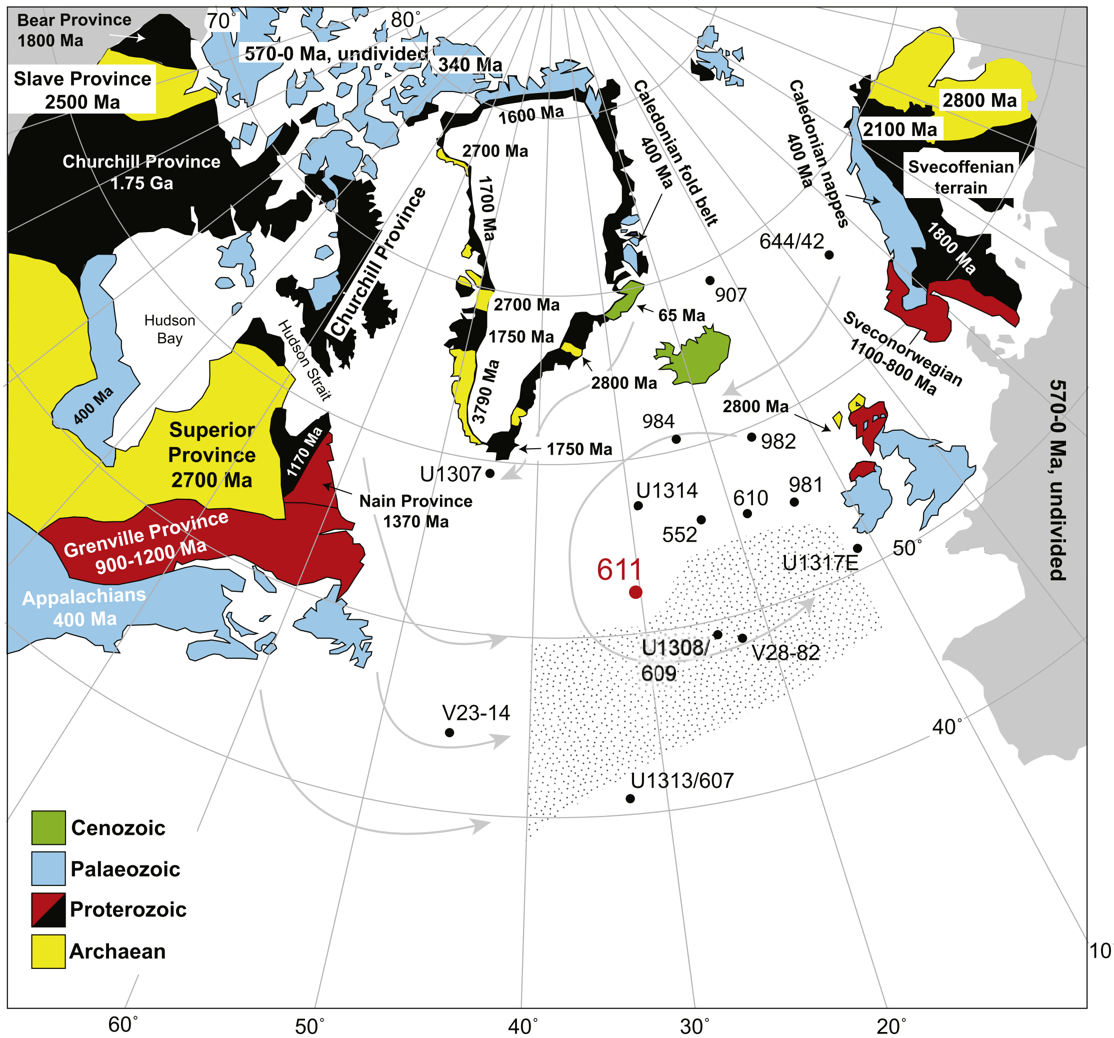

Fig. 1. North Atlantic Ocean and generalised surrounding continental geology (and stratigraphic ages). Also shown are the locations of DSDP Site 611 and other sites discussed in the main text. Arrows denote simplified, mean paths of icebergs during the Last Glacial based on suggestions by Ruddiman (1977) and De'Ath et al. (2006). The stippled area represents approximate position of (>63 μm < 2 mm non-carbonate) Last Glacial maximum (25–13 ka) coarse lithic flux (>250 mg cm^{-2} ka^{-1}) to the subpolar North Atlantic Ocean (Ruddiman, 1977), following Hemming (2004). Geological map redrawn from Gwiazda et al. (1996a).

in the Nordic Seas (e.g. Jansen et al., 1990; Jansen and Sjøholm, 1991; Fronval and Jansen, 1996) and subpolar North Atlantic Ocean (e.g. Shackleton et al., 1984; Ruddiman and Raymo, 1988; Raymo et al., 1989, 1992), Maslin et al. (1998) proposed that major ice-sheet expansions on Greenland and Scandinavia at ∼2.72 Ma led the maturation of continental ice on Northeast America by ∼200 ka. Their suggestion was based on the observation that whilst IRD inputs to the Iceland and Vøring Plateaus in the Nordic Seas (at ODP Sites 907 and 664, respectively) increased significantly during MIS G6, IRD deposition in North Atlantic Ocean (at DSDP Sites 552A, 607 and 609) appeared to have been relatively low until MIS 100, 2.52 Ma, the first large amplitude (∼+1.1‰ VPDB relative to present) obliquity-paced benthic δ^{18}O glacial cycle during iNHG. It is now known, however, that MIS G6-103 (2.75–2.55 Ma) was lost from the stratigraphy of Site 552A in a core break (Raymo et al., 1989). Subsequent generation of higher-resolution (Kleiven et al., 2002) records of ice-rafting to North Atlantic Ocean DSDP Sites 607 and 610 (Fig. 1b and c), also led Kleiven et al. (2002) to suggest that IRD deposition in the northern hemisphere during MIS G6 instead reflects a synchronous expansion of ice-sheets on Greenland, Scandinavia and Northeast America to their marine-calving margins from 2.72 Ma, during what is now commonly referred to as the onset of major NHG (e.g. Sigman et al., 2004; Haug et al., 2005; Etourneau et al., 2010).

It is important to understand what the onset of abundant IRD deposition in the North Atlantic Ocean during MIS G6 means in terms of ice-sheet extent because the sequence in which different ice sheets mature can be used to help test competing hypotheses for the triggering of, and feedback process involved in, cryosphere expansion in the northern hemisphere. Abundant marine geophysical (e.g. Geissler and Jokat, 2004; Sarkar et al., 2011) and terrestrial geological (e.g. Einarsson and Albertsson, 1988; Geirsdóttir and Eiríksson, 1994) evidence confirms that circum-Nordic Sea landmasses were extensively glaciated during MIS G6. Assessing the magnitude of glacial expansion on North America and its relative contribution to the onset of abundant iceberg rafting to the North Atlantic Ocean from 2.72 Ma is more challenging, however, because icebergs calved from Greenland and other European ice-sheets serve as potential additional, and perhaps even the dominant, sources of abundant IRD to the North Atlantic at this time (Bailey et al., 2012).

To shed new light on when North America first became a significant contributor of IRD to the subpolar North Atlantic Ocean during iNHG, and to improve our understanding of what the onset of abundant IRD inputs to this region during MIS G6 means in terms of ice-sheet extent, we report the first detailed study of the provenance of sand-sized IRD deposited in the North Atlantic between MIS G6 and MIS 100 (~2.72–2.52 Ma) determined from the Pb-isotope ratios of ~300 individual ice-rafted feldspars deposited at Deep Sea Drilling Program (DSDP) Site 611 (~53°N).

2. History of ice-rafting and IRD deposition associated with iNHG

Our understanding of the history of Cenozoic NHG has improved substantially over the past three decades (e.g. Prell, 1984; Shackleton et al., 1984; Raymo et al., 1989; Jansen and Sjøholm, 1991; Raymo et al., 1992; Haug and Tiedemann, 1998; Maslin et al., 1998; Jansen et al., 2000; Kleiven et al., 2002; Haug et al., 2005; Lisiecki and Raymo, 2005; Mudelsee and Raymo, 2005; Eldrett et al., 2007; Lunt et al., 2008; Thierens et al., 2012). Based largely on the occurrence of sand-sized IRD in marine sediments, we now know that the glacial history of Greenland and other circum-Arctic Ocean landmasses is long-lived and extends back to at least 38 Ma (Eldrett et al., 2007; Backman and Moran, 2008), but that there is no sedimentary evidence in the Norwegian Sea (on the Vøring Plateau) for extensive iceberg calving and presumably significant ice-sheet growth on Southern Scandinavia until ~2.72 Ma (Krissek, 1989; Henrich and Baumann, 1994; Jansen et al., 2000).

The onset of major IRD deposition on the Vøring Plateau at ~2.72 Ma (MIS G6, Fig. 2K) is broadly coincident with IRD-based evidence at Site 907 (on the Iceland Plateau, Fig. 2J, Jansen et al., 2000) and Site U1307 on the North Atlantic Ocean Eirik Drift (Fig. 2I, Sarnthein et al., 2009) for expansion of the Greenland Ice Sheet at that time. Both land-based evidence for major glacial expansion on Iceland (Geirsdóttir and Eiríksson, 1994) and marine geophysical (Geissler and Jokat, 2004; Sarkar et al., 2011) and IRD-based evidence for expansion of ice on Svalbard and in the Barents Sea region (Knies et al., 2009) also date to ~2.72 Ma. IRD found in sediments deposited on the Hebridean Slope off Northwest Britain (Stoker et al., 1994) and on the Porcupine Mounds off Southwest Ireland (Thierens et al., 2012) demonstrate that ice-caps likely existed on Great Britain and Ireland from at least ~2.6 Ma.

Continental ice sheets probably existed somewhere on North America during glacials from 2.72 Ma (Fig. 2C, Naafs et al., 2012), but it does not necessarily follow that expansion of continental ice in this region was dominantly responsible for, or even contributed to, the large increase in IRD inputs to the North Atlantic Ocean during MIS G6. Based on terrestrial evidence in the form of glacial tills, we can be confident that a major North American Laurentide Ice Sheet expanded to the middle latitudes (to ~39°N in Missouri) during MIS 100, 98 and 96 (Fig. 2E, Balco and Rovey, 2010). The lack of any terrestrial (Balco and Rovey, 2010) and marine-proximal (e.g. Joyce et al., 2003; modified to timescale of Cande and Kent, 1995) evidence for widespread glaciation of North America prior to ~2.5 Ma, raises the possibility, however, that a Northeast American Ice Sheet may not have matured sufficiently to be a significant source of icebergs and IRD to the subpolar North Atlantic Ocean until MIS 100, the oldest glaciation for which global sea level is convincingly shown to have fallen by at least ~60 m relative to present (Naish, 1997; Miller et al., 2012). By contrast, lowest-end estimates of global sea-level fall during MIS G6, 2.72 Ma, span only ~13–35 m relative to present (Bintanja and van de Wal, 2008; Miller et al., 2012). It is instructive to determine, therefore, the extent of continental ice-sheets in the northern hemisphere during MIS G6 when IRD inputs to the subpolar North Atlantic Ocean first increased dramatically, above their background (trace) values, but global benthic δ^{18}O, on average, was ~0.3‰ lower than in MIS 100.

IRD fluxes have only been shown to increase significantly at 2.72 Ma in the northeast Atlantic Ocean at ODP Sites 984 (Fig. 2H; Bartoli et al., 2006) and 982 (Fig. 2G; Baumann and Huber, 1999; Bolton et al., 2011) at DSDP Site 610 (Fig. 2F; Kleiven et al., 2002) and at Integrated Ocean Drilling Program (IODP) Site U1314 (Hayashi et al., 2010). Further south, IRD inputs (at latitudes <52°N) during MIS G6 were extremely low. In contrast to MIS 100 (Bailey et al., 2012) only trace amounts of IRD are found in sediments deposited at Site 609 (Fig. 2E, Raymo et al., 1989) and its reoccupation, IODP Site U1308 (Fig. 2E, Bailey et al., 2010), at the centre of the Last Glacial North Atlantic Ocean IRD belt (Ruddiman, 1977). On the southerly limit of the Last Glacial IRD belt, similarly low numbers of IRD are found at Site 607 (Fig. 2D, Raymo et al., 1989; Bolton et al., 2010). The spatial pattern of IRD deposition in the North Atlantic is ultimately a function of iceberg survivability. The concentration of IRD inputs to the northeastern sector of the Atlantic Ocean during MIS G6 and presence of only trace numbers of IRD in sediments deposited during MIS G6 south of ~52°N highlights the possibility, however, that the onset of 'major ice-rafting' to the North Atlantic at 2.72 Ma may have been more the product of enhanced glaciation of Greenland and other circum-Nordic Sea landmasses rather than a major expansion of a North American ice-sheet to its marine margin.

3. Study site and methods

3.1. Site 611

Site 611C was drilled during DSDP Leg 94 on the lower eastern flank of the Reykjanes Ridge on the Gardar Drift (at ~3200 m depth), near the Charlie-Gibbs Fracture Zone (~52°5′N; 30°2′W, Fig. 1). We selected Hole 611C because, unlike more southerly records, its sediments contain abundant IRD deposited during glacials from MIS G6 (see Section 2). Previous Pb-isotope data for MIS 100 from Hole 611A (Bailey et al., 2012) also reveal that this site is well situated to receive IRD from the full range of potential major continental northern hemisphere ice-sheets during iNHG.

3.2. Sampling and age model generation

To improve our understanding of IRD deposition and its provenance at Site 611 and to capture the onset of abundant IRD deposition in the subpolar North Atlantic Ocean during MIS G6, we sampled Hole C at Site 611 guided by the shipboard-derived palaeomagnetic reversal stratigraphy and split-core images (Shipboard Scientific Party, 1987). We sampled all sections between 15H 1W and 16H 5W at ~10 cm resolution. Generation of a new composite benthic oxygen isotope stratigraphy, by combining Hole 611A (Bailey et al., 2012) and Hole 611C (this study) data, and its comparison to the global benthic δ^{18}O stack, the LR04 (Lisiecki and Raymo, 2005) confirms our samples span MIS G9 to 99 (~2.8–2.5 Ma, Fig. 3; see supplementary information).

3.3. Stable isotope measurements

Stable isotope data (δ^{18}O) were generated for Hole 611C on the benthic foraminiferal calcite of species separates of *Cibicidoides wuellerstorfi* ($n = 80$ samples) picked from the >212 μm sediment fraction over 118.2–135.05 m below sea floor (mbsf). Typically, 1–5 tests were analysed per sample. Stable isotope measurements were made at the National Oceanography Centre using a Europa GEO 20–20 mass spectrometer equipped with an automatic carbonate preparation system. Data are reported relative to the Vienna Pee Dee Belemnite (VPDB) standard with an external analytical

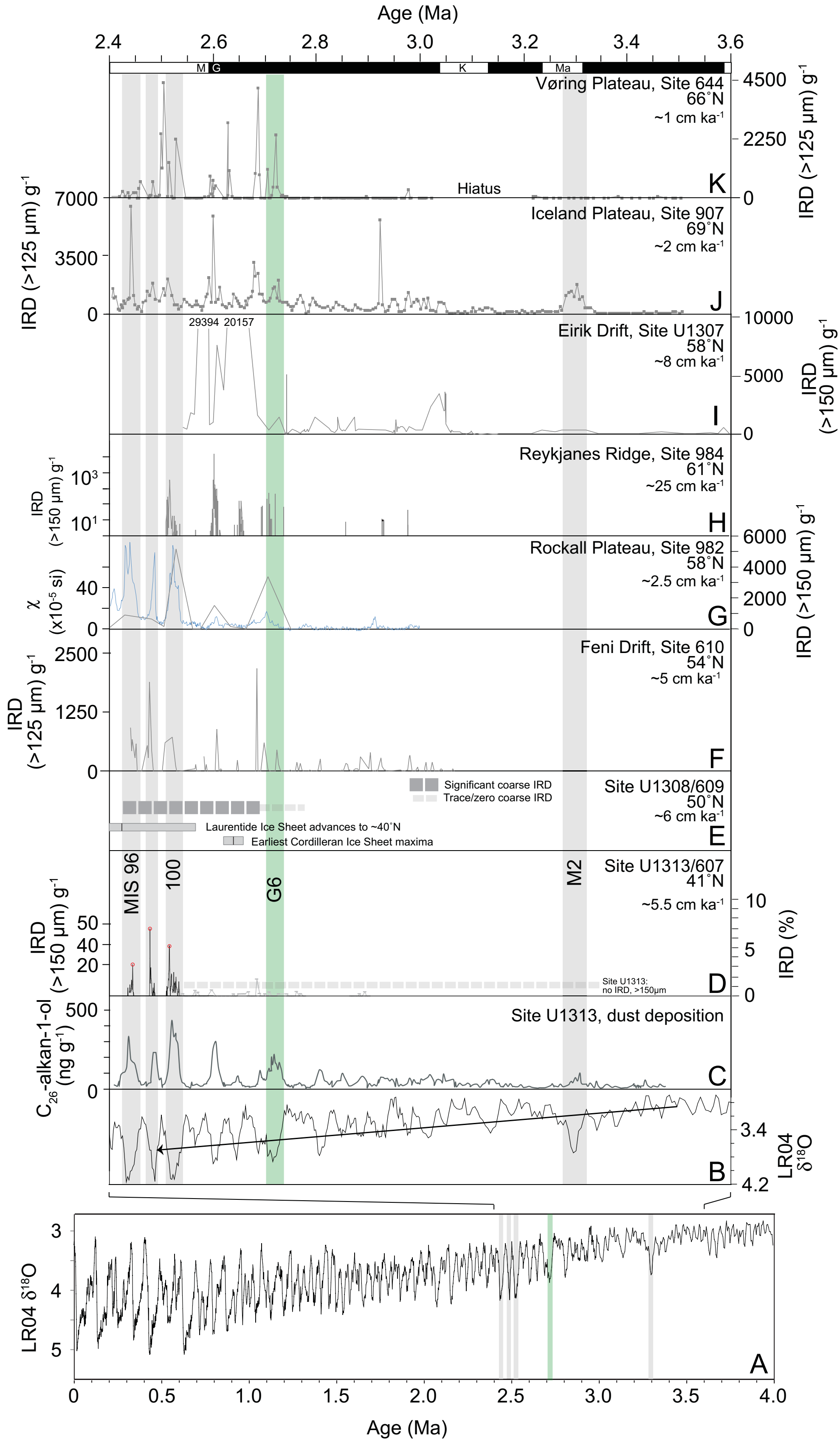

Fig. 2. LR04 global benthic $\delta^{18}O$ stack (**A & B**; Lisiecki and Raymo, 2005); concentration of the long-chain alkan-1-ol in sediments from IODP Site U1313 (**C**), used as a proxy for glacially derived North American aeolian dust inputs to the North Atlantic Ocean by Naafs et al. (2012); Late Pliocene–early Pleistocene coarse lithic IRD records from the North Atlantic Ocean at (**D–E**) DSDP Sites 607 (% 'coarse' sand, light grey; Kleiven et al., 2002) and 609 (Raymo et al., 1989) and their reoccupations IODP Sites U1313 (% IRD >150 μm, black line and red spot data for IRD, >150 μm g^{-1} dry sediment; Bolton et al., 2010) and U1308 (Bailey et al., 2010), (**F**) DSDP Site 610 (Kleiven et al., 2002), (**G**) ODP Site 982 shipboard

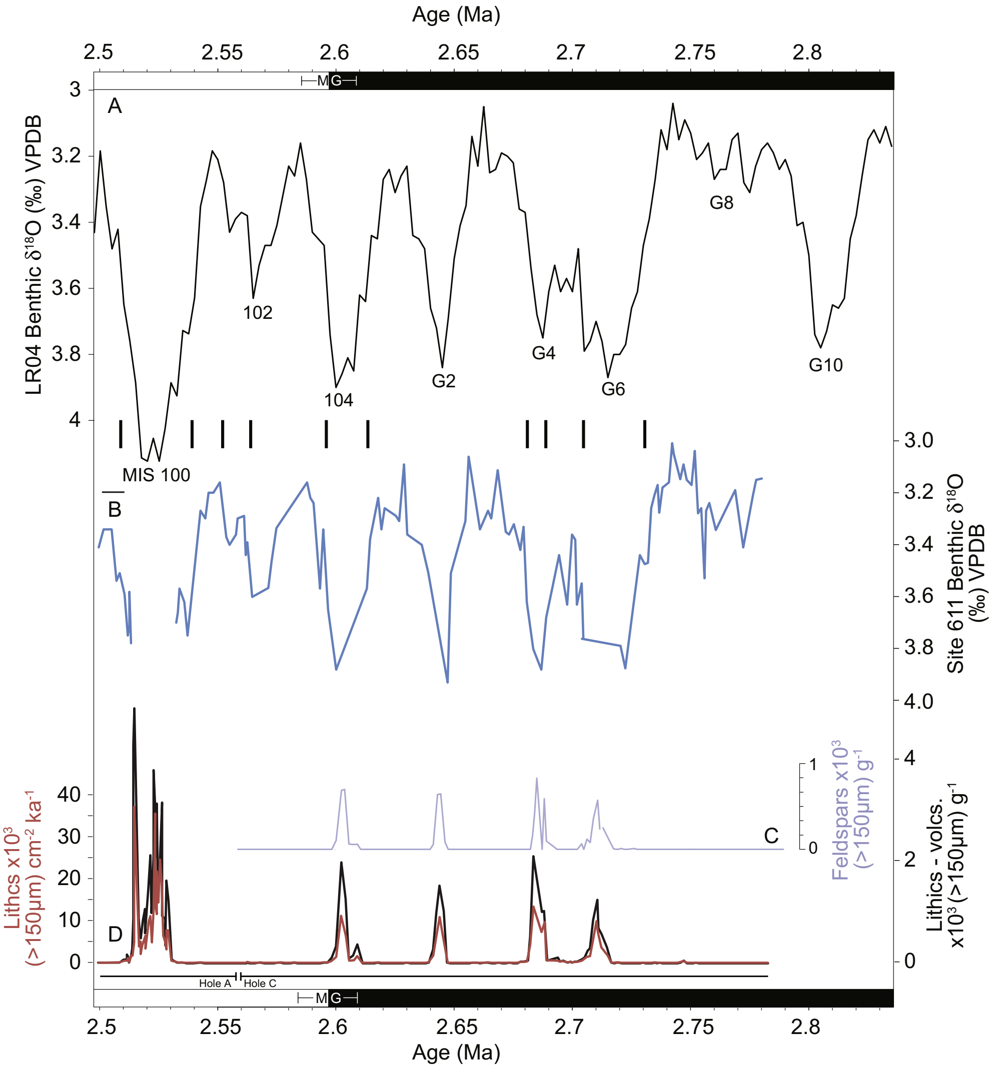

Fig. 3. Pliocene Palaeoceanographic records versus age: **(A)** Stack of globally representative benthic $\delta^{18}O$ (the 'LR04'; Lisiecki and Raymo, 2005); **(B)** Site 611 benthic $\delta^{18}O$ measured on epifaunal species *C. wuellerstorfi* (this study and Bailey et al., 2012); **(C)** coarse feldspar abundance (blue line); **(D)** coarse lithic abundance (black line) and flux (red line) (both minus volcanic glass). IRD composition is comparable to that reported for MIS 100 Site 611A IRD (Bailey et al., 2012). Short vertical black lines denote tie points between Site 611 and LR04. All Site 611 data is displayed as a composite of Hole A and C data (see supplementary information). Hole A benthic $\delta^{18}O$ data (Bailey et al., 2012) adjusted by −0.2‰ relative to benthic $\delta^{18}O$ data from Hole C (this study) to account for an analytical offset generated by the mass spectrometers used in the respective studies. Numbers of benthic foraminifera in drift sediments (such as those deposited at Site 611) are commonly low. Whilst numbers of benthic foraminifer a picked in this study permit the generation of a benthic $\delta^{18}O$ stratigraphy that allows us to identify all glacial–interglacial cycles in our target interval, our record does not resolve orbital $\delta^{18}O$ cycles with sufficient fidelity to provide two tie points per obliquity (inter)glacial cycle. To avoid over tuning our record to the LR04 we only use ten tie points. This results in an average sedimentation rate of ~7.5 cm ka^{-1}. The black/white bars at the top/bottom of the figure denote age of Gauss (G)/Matuyama (M) chronozone boundary (2.581 Ma; Shipboard Scientific Party, 1987; Cande and Kent, 1995). (For interpretation of the references to colour in this figure legend, the reader is referred to the web version of this article.)

precision, based on replicate analysis of an in-house standard calibrated to NBS-19, of 0.065‰ (1σ). *C. wuellerstorfi* $\delta^{18}O$ values were adjusted for species-specific offsets relative to calcite precipitated in equilibrium with seawater by adding +0.64‰ (Shackleton and Hall, 1984).

3.4. Coarse lithic counts

The concentration of lithic grains (>150 µm) per gram of dry sediment was estimated at Hole 611C for our study interval using a standard method (Bond and Lotti, 1995). We counted a

magnetic susceptibility (blue line, Shipboard Scientific Party, 1996) and coarse lithic abundance (grey line, Baumann and Huber, 1999); **(H)** ODP Site 984 (Bartoli et al., 2006) and **(I)** IODP Site U1307 (Sarnthein et al., 2009); IRD records from Nordic Seas at **(J)** ODP Site 907 (Jansen et al., 2000) and **(K)** ODP Site 644 (Jansen and Sjøholm, 1991); Also shown in (D) are age ranges (age = black vertical line at centre of rectangle, rectangle width = 2σ uncertainty) for the oldest cosmogenically-dated Laurentide Ice Sheet advance into central Missouri, USA (Balco and Rovey, 2010) and earliest and most extensive Cordilleran Ice Sheet in northwest North America (Hidy et al., 2013). Long black arrow in (B) depicts ~1000 ka-long ramp in benthic $\delta^{18}O$ identified by Mudelsee and Raymo (2005). Horizontal green bars indicate the 'onset of major NHG' across marine isotope stage (MIS) G6 (e.g. Haug et al., 2005). Vertical grey bars denote glacial MIS M2, 100, 98 and 96. The black/white bars at top of figure denote palaeomagnetic chronozone boundaries (Cande and Kent, 1995): M = Matuyama, G = Gauss, K = Keana and Ma = Mammoth. Unavailability of dry bulk density data for many DSDP/ODP records presented here prohibits estimates of meaningful coarse lithic fluxes at many of these sites. Average Pliocene sedimentation rates shown for each record illustrate, however, that our assertion that large IRD inputs during MIS G6 are limited to the northeast North Atlantic Ocean (i.e. north of Site U1308) is not a function of plotting relative abundance data. Age models taken from the respective studies (but all stratigraphies presented consistent with ages assigned to the polarity-chronozone stratigraphy of Cande and Kent, 1995). Site 984 IRD data in (H) plotted on log scale for clarity. (For interpretation of the references to colour in this figure legend, the reader is referred to the web version of this article.)

minimum of 300 grains in each sample. These data were combined with data from Hole 611A (for MIS 102-99; Bailey et al., 2012) to produce a composite record of ice-rafting to Site 611 spanning MIS G9 to MIS 99. Coarse lithic fluxes were estimated following Peck et al. (2007) using dry bulk densities determined from oven dried bulk samples and sedimentation-rates based on our age-model.

3.5. Lead isotope measurements on individual ice-rafted feldspar

To improve our understanding of the provenance of IRD deposited in the subpolar North Atlantic during iNHG we measured the Pb-isotope composition of 198 sand-sized (>150 μm) ice-rafted feldspars (Table 1) deposited at Site 611 during glacial maxima (full glacial, FG) of MIS G6, G4, G2 and 104 and during the onset of IRD deposition (early glacial, EG) during MIS G6 to compliment previously published ice-rafted feldspar Pb-isotope data for EG ($n = 29$) and FG ($N = 78$) MIS 100 from this site (Bailey et al., 2012). All feldspar Pb-isotope analyses were performed at the National Oceanography Centre Southampton using a ThermoFinnigan Neptune multicollector inductively coupled plasma mass spectrometer (MC-ICP-MS) coupled with a NewWave/ESI UP193fx homogenised ArF excimer laser ablation system, operating at 193 nm and using a 150 μm spot, following the analytical protocols of Bailey et al. (2012) (also see supplementary information).

Pb isotope studies of North Atlantic Ocean terrigenous sediments are well established as a tracer of IRD (e.g. Gwiazda et al., 1996a,b; Fagel et al., 2002; Farmer et al., 2003; Colville et al., 2011; Bailey et al., 2012; Maccali et al., 2012). Its application as a provenance tool utilises systematic differences in the regional geology of circum-North Atlantic Ocean landmasses, which vary as a function of age and tectonic (metamorphic) history (Fig. 1). To determine the provenance of our feldspars, we compared their Pb-isotope compositions to those of potential circum-North Atlantic Ocean tectonic terranes as defined by Bailey et al. (2012). We focused on the Pb-isotope composition of potential circum-North Atlantic Ocean Pb-isotope terrane fields (Fig. 1) in $^{206}Pb/^{204}Pb$–$^{207}Pb/^{204}Pb$ space and in $^{206}Pb/^{204}Pb$–$^{208}Pb/^{204}Pb$ space (Fig. 4).

The isotopic composition of potential terrane sources for North Atlantic IRD can show a relatively high degree of overlap in $^{206}Pb/^{204}Pb$–$^{207}Pb/^{204}Pb$ and $^{206}Pb/^{204}Pb$–$^{208}Pb/^{204}Pb$ space (Fig. 4; Bailey et al., 2012). To aid interpretation of the meaning of the onset of abundant IRD deposition in the North Atlantic Ocean at 2.72 Ma, we therefore also compared our new datasets from MIS G6-104 to previously published Pb-isotope data for ice-rafted feldspars deposited at Site 611 during MIS 100, 2.52 Ma, (Bailey et al., 2012) and during MIS 2 (~23 ka) at the centre of the Last Glacial IRD belt at DSDP Site 609 (Bailey et al., 2012) and near-by site VM28-82 (Gwiazda et al., 1996a).

Table 1
Sampling guide for ice-rafted, sand-sized feldspars analysed in this study.

Site	Sample I.D.	MIS	Number of analyses[a]
DSDP 611A (FG)	12H 2W 133–134 & 143–144 cm 12H 3W 8–11 cm	100	78[b]
DSDP 611A (EG)	12H 3W, 96–98 cm	100	29[b]
DSDP 611A (FG)	13H 2W, 52–53.5 cm	104	30
DSDP 611C (FG)	15H 5W, 35–36.5 cm	G2	50
DSDP 611C (FG)	15H 7W, 5–6.5 cm	G4	43
DSDP 611C (FG)	16H 2W, 4–5 cm	G6	49
DSDP 611C (EG)	16H 2W, 40–41.5 cm	G6	26

[a] Total number of analyses = 305 (198 new data presented in this study). EG and FG refer to early and full glacial time intervals, respectively.
[b] Data from Bailey et al. (2012).

4. Results and discussion

4.1. Flux of North Atlantic IRD deposited at Site 611 during iNHG

Our new record of the concentration and flux of coarse lithics (>150 μm) at Hole 611C (for MIS G9–MIS 102, this study) is plotted together with previously published coarse lithic data from Hole 611A (MIS 102–MIS 99; Bailey et al., 2012) as a composite record of IRD inputs to Site 611 between MIS G9 and MIS 99 (2.85–2.5 Ma) in Fig. 3D. Previously, Bailey et al. (2012) demonstrated that flux of IRD to Site 611 during MIS 100 (~10–20,000 grains, >150 μm, cm^{-2} ka^{-1}) was on the same order of magnitude to those observed for the north Atlantic Ocean during the Last Glacial (e.g. Bond et al., 1992). Our new coarse lithic counts for Hole 611C, which extend our understanding of IRD inputs to Site 611 back to MIS G9, highlight that Last Glacial magnitude IRD deposition rates existed at this site during glacials from MIS G6 onwards.

4.2. Provenance of North Atlantic IRD deposited at Site 611 during iNHG

Having established that Quaternary magnitude fluxes characterize IRD deposition at Site 611 during glacials since MIS G6, 2.72 Ma, next we consider the provenance of this ice-rafted material using our new (MIS G6-104) and previously published (MIS 100; Bailey et al., 2012) Pb-isotope analyses of individual sand-sized feldspars from this site. The Pb-isotope composition of individual sand-sized (>150 μm) feldspars deposited at Site 611 during EG MIS G6 and FG MIS G6-104 (this study, $n = 26$ and 172, respectively) together with previously published EG and FG MIS 100 data from this site ($n = 107$; Bailey et al., 2012) and EG MIS 100 data from Site U1308 ($n = 58$; Bailey et al., 2012) are shown in Figs. 5 and 6.

A histogram of $^{206}Pb/^{204}Pb$ ratios of all ambient glacial North Atlantic ice-rafted feldspars analysed for iNHG (this study; Bailey et al., 2012) and for the Last Glacial (Gwiazda et al., 1996a; Bailey et al., 2012) reveals six distinct modes centred on $^{206}Pb/^{204}Pb$ ratios of ~12.6, 13.4, 14.8, 15.7, 17.2 and 18.2 (termed Mode I, II, III, IV, V and VI, respectively; Fig. 7) that are associated in turn with progressively increased $^{207}Pb/^{204}Pb$ and $^{208}Pb/^{204}Pb$ ratios (Figs. 5 and 6). At Site 611, early glacial IRD deposition during MIS G6 (Figs. 5L and 6L) and MIS 100 (Figs. 5K and 6K) is dominated by feldspars with compositions akin to Mode I, II, III and IV. In contrast to these EG ice-rafting events, the modal distribution of feldspars deposited during full glacial conditions at Site 611 during iNHG in $^{206}Pb/^{204}Pb$ space is more variable (Fig. 5A–I, 6A–I).

A large range of Pb isotope compositions are observed for our iNHG full glacial time windows, which are all characterised by feldspars with compositions akin to Mode I through VI. A histogram of $^{206}Pb/^{204}Pb$ ratios of FG MIS G6 feldspars, however, illustrates that this population is dominated by Mode I, II and IV (Figs. 5I and 6I). Compared to MIS G6, our MIS G4 population contains fewer Mode II feldspars and a higher proportion of Mode VI grains (Figs. 5H and 6H). Yet, it is not until MIS G2, 2.64 Ma, that feldspars deposited during full glacial conditions at Site 611 are dominated by Mode VI grains (compare Figs. 5F–E and C, and 6F–E and C). Whilst the Pb-isotope composition of ice-rafted feldspars deposited at our study site during FG MIS G6-100 is diverse, the other primary observation that can therefore be made on the basis of these data is that the provenance of IRD delivered to Site 611 at this time was not constant.

4.2.1. Early glacial ice-rafting sources during late Pliocene and earliest Pleistocene iNHG

The majority (~80%, $n = 21$) of feldspars deposited at Site 611 during EG MIS G6 belong to Mode I, II and III (Fig. 5J,L). On the basis

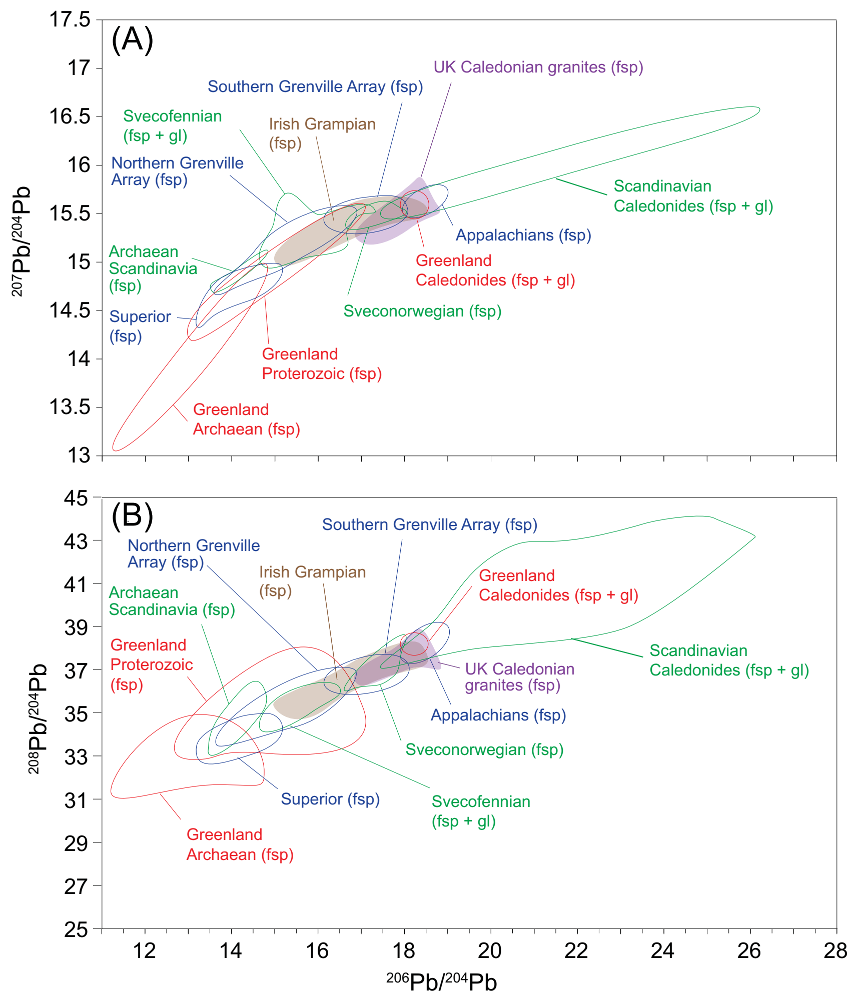

Fig. 4. Pb-isotope values for potential North Atlantic ice-rafted debris sources complied by Bailey et al. (2012): in ^{206}Pb/^{204}Pb–^{207}Pb/^{204}Pb space **(A)**, and in ^{206}Pb/^{204}Pb–^{208}Pb/^{204}Pb space **(B)**. The source fields are based on Pb-isotope composition of feldspars and conformable ore galenas from circum-North Atlantic Ocean bedrock. For details of the method and data citations, see Bailey et al. (2012). 'Fsp' and 'gl' refer to feldspar and galena, respectively, and represent the mineral separates on which the respective Pb-isotope analyses were performed.

of their ^{206}Pb/^{204}Pb, ^{207}Pb/^{204}Pb and ^{208}Pb/^{204}Pb ratios, ten of these grains (38% of the total population) can be unambiguously traced to the Archaean and late Proterozoic basements of Greenland. The Pb-isotope composition of the remaining Mode II and III grains (with ^{206}Pb/^{204}Pb ratios $>$ 13) also overlap with the Proterozoic field of Greenland and/or the Archaean Superior province of North America. The lack of significant numbers of feldspars that cluster about the Pb-isotope composition of the North American Churchill, southern Grenville and/or Appalachian terranes, all of which physically separate the Superior province from the North Atlantic Ocean, indicates that many of these Archaean and late Proterozoic feldspars were probably sourced from Greenland and not North America.

The overlap between the Pb-isotope compositions of potential source regions means that it is not possible to unambiguously identify the provenance of the minor numbers of Mode IV and VI feldspars ($\sim$19%, $n = 5$) that characterize EG MIS G6 IRD at Site 611 (Figs. 5J,L and 6J,L). Of the potential source regions, Mode IV feldspars overlap in both ^{206}Pb/^{204}Pb–^{207}Pb/^{204}Pb and ^{206}Pb/^{204}Pb–^{208}Pb/^{204}Pb space with the Pb-isotope composition of Proterozoic Greenland bedrock and Scandinavian Svecofennian and Irish Grampian terranes. On the basis of their ^{208}Pb/^{204}Pb ratios, Mode VI feldspars ($n = 2$) could be sourced from the British Isles and/or the Caledonian Scandinavian or North American Appalachian terranes. Regardless, the overall provenance of our EG MIS G6 feldspars, which bears a strong resemblance to that previously reported for feldspars deposited at Site 611 and Site U1308 during EG MIS 100 (black and grey data, respectively, in Fig. 5J; Bailey et al., 2012), supports the notion that IRD deposited in the North Atlantic during early glacial ice-rafting episodes of glaciations during iNHG is dominantly sourced from Greenland.

4.2.2. Full glacial ice-rafting sources during late Pliocene and earliest Pleistocene iNHG

Compared to MIS 100, a less distinct change occurs in the distribution of MIS G6 feldspars in ^{206}Pb/^{204}Pb–^{207}Pb/^{204}Pb and ^{206}Pb/^{204}Pb–^{208}Pb/^{204}Pb space between EG and FG populations (compare black data in Figs. 5A,J and 6A,J to blue data in Figs. 5G,J and 6G,J). In terms of their ^{206}Pb/^{204}Pb ratios, FG MIS G6 feldspars are still dominated by Mode I and II grains (41%, $n = 20$), but also now contain higher numbers of Mode III and IV grains (39%, $n = 19$).

On the basis of their Pb isotope compositions, a high proportion of FG MIS G6 feldspars (22%, $n = 11$; mainly Mode I and II) can be traced to the Archaean and late Proterozoic basements of Greenland (Figs. 5G and 6G). It is not possible to unambiguously

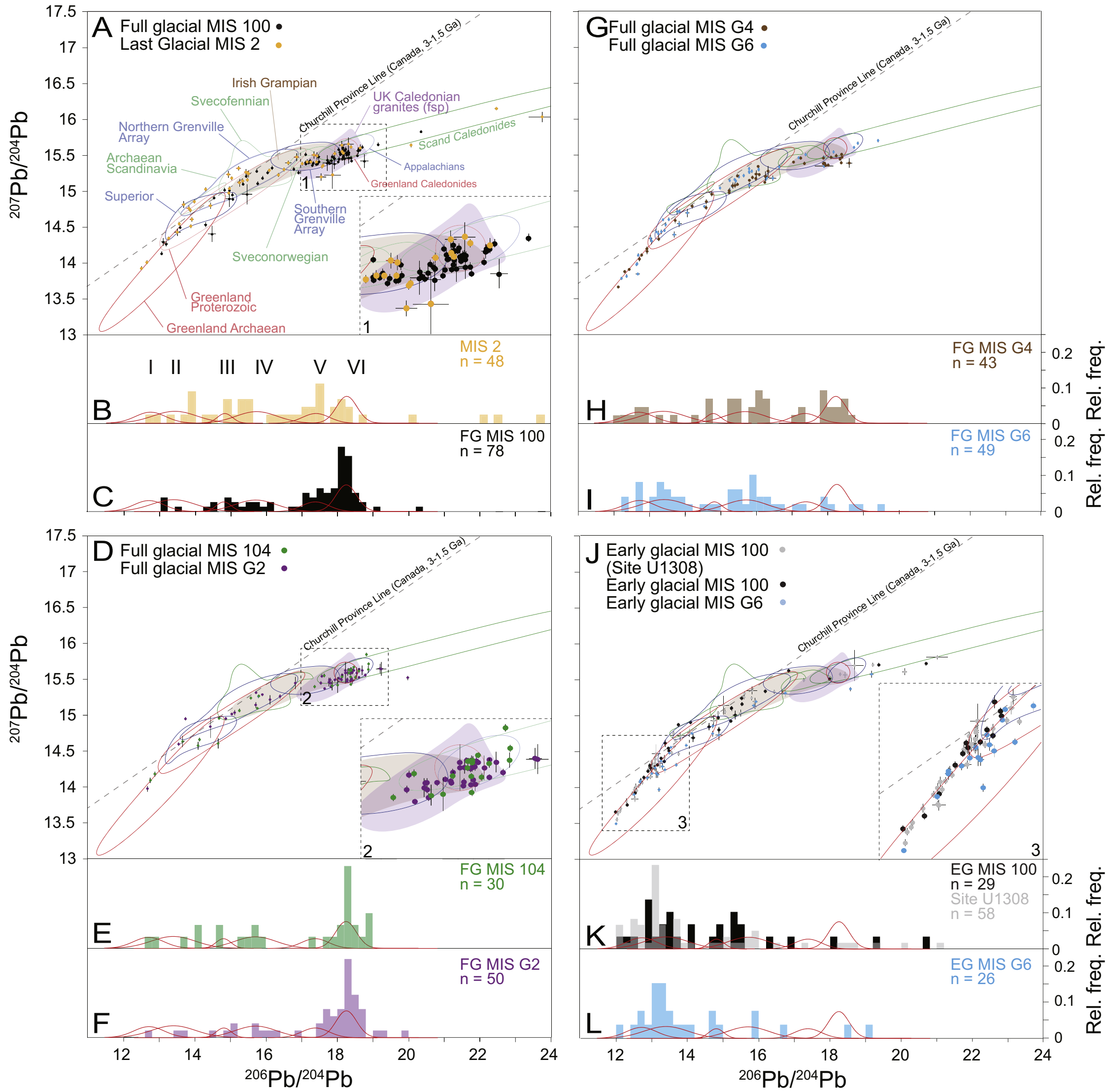

Fig. 5. The Pb-isotope composition (^{206}Pb/^{204}Pb vs. ^{207}Pb/^{204}Pb) of individual sand-sized (>150 μm) ice-rafted feldspars deposited at DSDP Site 611 during full glacial (FG) MIS 100 (**A**), MIS 104 and MIS G2 (**D**), MIS G4 and MIS G6 (**G**) and during early glacial (EG) MIS 100 and MIS G6 (**J**). Also shown are histograms of their ^{206}Pb/^{204}Pb ratios (in **B, C, E, F, H, I, K** and **L**) and the range of Pb-isotope values for potential ice-rafted debris sources (see Fig. 4a). Red normal distribution profiles on histograms denote the six modes (I, II, III, IV, V and VI) fitted graphically to ^{206}Pb/^{204}Pb values shown in Fig. 7. (For interpretation of the references to colour in this figure legend, the reader is referred to the web version of this article.)

identify the provenance of the remaining feldspars in this population (mainly from Mode II, III and IV), but many of these grains could be derived from Proterozoic Greenland terranes, the British Isles, the Scandinavian Svecofennian terrane and/or the North American Superior and Northern Grenville provinces. The absence of significant numbers of feldspars that overlap with either Pb-isotope compositions of the North American Southern Grenville, Churchill or Appalachian terranes, but also the Scandinavian Sveconorwegian and Caledonian terranes, highlights, however, that some of these Mode II–IV grains are probably also derived from Proterozoic-aged rocks on Greenland (Figs. 5G and 6G).

The distribution of Site 611 feldspars in ^{206}Pb/^{204}Pb–^{207}Pb/^{204}Pb space and in ^{206}Pb/^{204}Pb–^{208}Pb/^{204}Pb space for FG MIS G6 and FG MIS G4 is highly comparable (Fig. 5G–I and 6G–I). The similarity of the Pb-isotope composition of feldspars deposited at our study site during these time windows highlights the possibility that the provenance of IRD deposited at Site 611 during FG MIS G6 and FG MIS G4 is similar. Compared to FG MIS G6, the source(s) responsible for the deposition of Mode II feldspars at Site 611 during FG MIS G4 appear less important for this glacial (compare Fig. 5H–I). An increase in the importance of Mode VI feldspars highlights the possibility that the North American Appalachians may have become a more important source of IRD to our study site during MIS G4. Based on their ^{206}Pb/^{204}Pb–^{207}Pb/^{204}Pb and ^{208}Pb/^{204}Pb ratios, some or all of these grains could also be sourced from the British Isles or Caledonian Scandinavian and/or Greenland terranes (Figs. 5G and 6G). Regardless, a sizable portion ($\sim$16%, $n = 7$) of our FG MIS G4 feldspars can still be unambiguously attributed to the Archaean basement of Greenland (Figs. 5G and 6G).

The Pb-isotope composition of feldspars deposited at Site 611 during FG MIS G2 and FG MIS 104 bears a strong resemblance to previously published ice-rafted feldspar data for FG MIS 100 from this site (compare Figs. 5D–F to 5A, 5C and 6D–F to 6A, 6C; Bailey et al., 2012). Compared to FG MIS G6 and G4, a significant reduction is observed for FG MIS G2 in the number of Mode I and II feldspars that can be unambiguously attributed to the Archaean and late

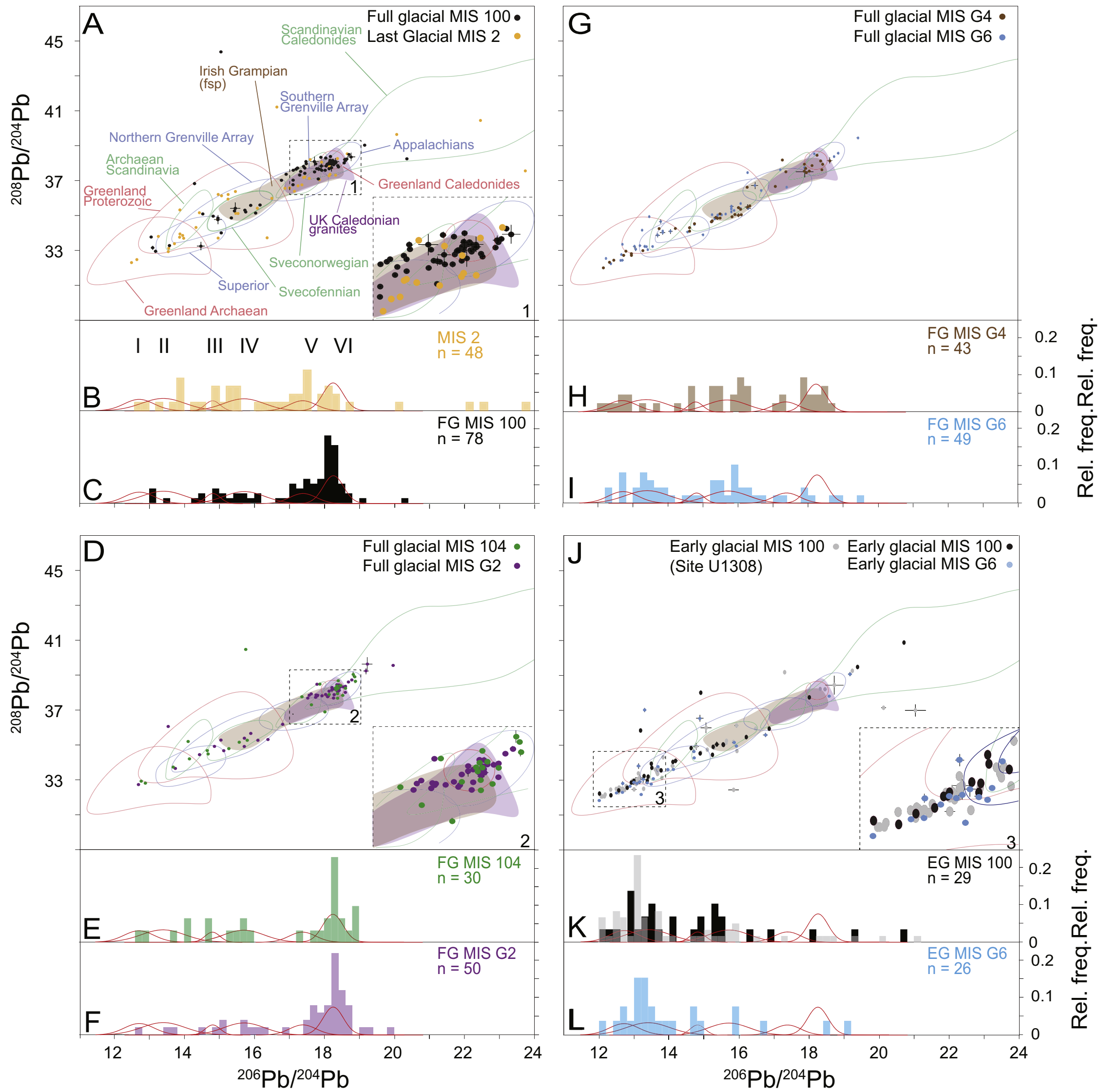

Fig. 6. The Pb-isotope composition ($^{206}Pb/^{204}Pb$ vs. $^{208}Pb/^{204}Pb$) of individual sand-sized (>150 μm) ice-rafted feldspars deposited at DSDP Site 611 during full glacial (FG) MIS 100 (**A**), MIS 104 and MIS G2 (**D**), MIS G4 and MIS G6 (**G**) and during early glacial (EG) MIS 100 and MIS G6 (**J**). Also shown are histograms of their $^{206}Pb/^{204}Pb$ ratios (in **B, C, E, F, H, I, K** and **L**) and the range of Pb-isotope values for potential ice-rafted debris sources (see Fig. 4b). Red normal distribution profiles on histograms denote the six modes (I, II, III, IV, V and VI) fitted graphically to $^{206}Pb/^{204}Pb$ values shown in Fig. 7. (For interpretation of the references to colour in this figure legend, the reader is referred to the web version of this article.)

Proterozoic basement of Greenland (respectively, 2% and 6%; $n = 1$ and 2; compare Fig. 5G–I to 5D,F). Compared to FG MIS 100, both FG MIS G2 and FG MIS 104 contain fewer Mode V feldspars (Figs. 5C and 5E–F). IRD deposited at Site 611 during FG MIS G2, 104 and 100 are, however, dominated by feldspars with compositions akin to Mode VI grains (respectively, 60%, 50% and 53%; $n = 30$, 15 and 41; Figs. 5A,C and D–F, 6A,C and D–F).

This shift towards a more radiogenic Pb-dominated population during FG MIS G2 likely highlights a notable dilution of the relative importance of Mode I–IV feldspars, and the Archaean and Proterozoic basement of Greenland, as a source of IRD to our study site by other circum-North Atlantic terranes. On the basis of their $^{206}Pb/^{204}Pb$, $^{207}Pb/^{204}Pb$ and $^{208}Pb/^{204}Pb$ ratios, the Mode VI feldspars deposited at Site 611 during glacials since MIS G2 may be sourced from late Proterozoic-aged North American terranes, Caledonian-aged North American and Greenland terranes, the Irish Grampian terrane and/or British and Irish granites (Figs. 5A,D and 6A,D).

4.3. The onset of abundant IRD deposition at DSDP Site 611, 2.72 Ma, was not dominated by iceberg calving sources from North America

It is hypothesised that the onset of abundant IRD deposition in the subpolar North Atlantic Ocean during MIS G6, 2.72 Ma, reflects a synchronous expansion of continental ice-sheets on Greenland, Scandinavia and Northeast America to their marine-calving margins (Kleiven et al., 2002) during what is now known as the onset of major NHG (e.g. Haug et al., 2005). If this hypothesis is correct, and that this template for ice-sheet expansion in the northern hemisphere characterised glaciations during iNHG from 2.72 Ma, then we might expect that the provenance of IRD deposited at Site 611 over the duration of our study interval would remain more or less constant. Our new Pb-isotope datasets for Site 611 show, however, that a persistent pattern in terms of IRD provenance is not established at this site until 2.64 Ma, during MIS G2.

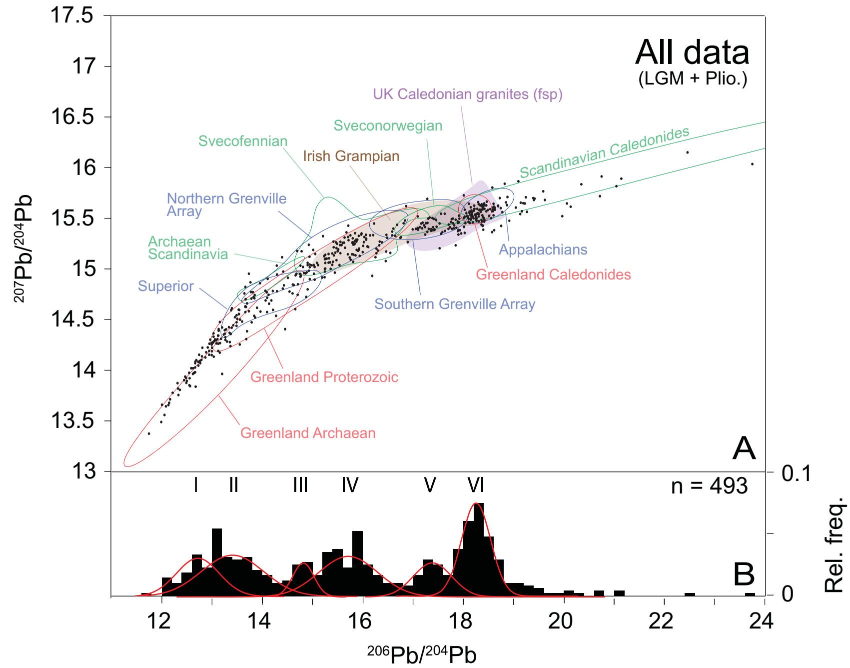

Fig. 7. Cross plot (^{206}Pb/^{204}Pb vs. ^{207}Pb/^{204}Pb, **A**) and histogram **(B)** of all Pb-isotope data available for ambient glacial subpolar North Atlantic Ocean ice-rafted feldspars (from Site 611 (this study and Bailey et al., 2012) and Sites 981, U1308 and 609 (Bailey et al., 2012), V28-82 and V23-14 (Gwiazda et al., 1996a)). Normal distribution profiles in red in (B) denote the six modes (I, II, III IV, V and VI) fitted graphically to this data. (For interpretation of the references to colour in this figure legend, the reader is referred to the web version of this article.)

The late Quaternary is undoubtedly characterised by major glaciation of the northern hemisphere to its middle latitudes (Clark and Mix, 2002). By Quaternary standards, the onset of 'major NHG' is, therefore, perhaps best defined by the first time during iNHG when northern hemisphere ice-sheets expanded into the middle latitudes (Head et al., 2008). Based on the terrestrial record of NHG, this condition appears to have been met in North America during MIS 100, 98 and 96 (Joyce et al., 2003; Balco and Rovey, 2010). Reconstructions of global sea-level for FG MIS 100 (Miller et al., 2012) and the similarity to the Last Glacial of the Pb-isotope composition of IRD deposited at Site 611 during this glacial (compare black and orange data in Figs. 5A and 6A) also support the notion that MIS 100 was associated with the growth of multiple, large northern hemisphere ice-sheets (Bailey et al., 2012). We therefore propose that the Pb-isotope composition of ice-rafted feldspars deposited at Site 611 during MIS 100 can be compared to our new datasets from this site to identify the existence of a glacial setting consistent with major, widespread NHG during glacials prior to MIS 100.

In our Pb–Pb plots, feldspars deposited at Site 611 during glacials since MIS G2 cluster about the Pb-isotope composition of late Proterozoic-aged North American terranes, Caledonian-aged North American and Greenland terranes, the Irish Grampian terrane and British and Irish granites (Figs. 5A,D and 6A,D). Given the overlap between potential source regions in Pb–Pb space (Fig. 4), our observation that the Pb-isotope signature of IRD at Site 611 associated with FG MIS 100 is first seen at this site during MIS G2 reflects three possibilities: 1) that continental ice on North America does not dominate IRD deposition at our study site until during MIS G2 at 2.64 Ma, 2) that the British and Irish Ice Sheet became an important source of IRD to Site 611 during MIS G2 (see Thierens et al., 2012), or 3) given the diverse age and Pb-isotope composition of Greenland's tectonic terranes (Fig. 3; Henriksen, 2008), the evolution of Pb-isotopes at Site 611 over our study interval may predominantly track changes in the dominant sources of icebergs calved from the Greenland Ice Sheet as it expanded during iNHG.

One possible reason why North American source(s) might not dominate the provenance of IRD deposited at Site 611 prior to MIS G2 is that even if North America was characterised by significant glaciation from 2.72 Ma, the Laurentide Ice Sheet eroded, but did not purge from this continent until 2.64 Ma a feldspar barren, pre glacial chemically-weathered regolith (see Clark and Pollard, 1998). Yet, based on our coarse lithic counts we can rule out this possibility, because the abundance of feldspars in glacial sediments deposited at Site 611 is consistently high between MIS G6 and 104 (Fig. 3C). An alternative explanation is that a larger proportion of our pre-MIS G2 Archaean and late Proterozoic grains were sourced from the Canadian Shield than we have argued for above.

Understanding the exact sources of IRD deposited at Site 611 during iNHG requires better characterization of the Pb-isotope composition of feldspars from IRD source regions and new provenance data from marine cores upstream of Site 611. Regardless, our new Pb-isotope datasets show that a persistent pattern of IRD provenance consistent at our study site with major NHG is not established at Site 611 during the onset of abundant IRD deposition in the subpolar North Atlantic Ocean at 2.72 Ma during MIS G6 (Figs. 2 and 3D; Kleiven et al., 2002), but rather ~80 ka later during MIS G2 (2.64 Ma). Continental ice existed somewhere on North America prior to MIS G2 (see Gao et al., 2012). We hypothesise, however, that IRD deposition in the open subpolar North Atlantic Ocean prior to 2.64 Ma was dominated by the melting of icebergs sourced from Greenland and other circum-Nordic Seas landmasses.

Our ideas need to be tested with new Pb-isotope datasets and other indicators of IRD provenance from subpolar North Atlantic Ocean records more proximal to, e.g. North America. Unfortunately, continuously cored late Pliocene records from the northwest Atlantic Ocean (which in this region are typically buried deeply beneath thick Pleistocene sequences) are not available. Our findings, therefore, strongly highlight the need for future ocean-drilling efforts to recover high fidelity Pliocene records from this region.

4.4. When did major NHG first occur during the Plio–Pleistocene?

If IRD deposition in the North Atlantic Ocean prior to ~2.64 Ma was dominated by iceberg calving from Greenland and other circum-Nordic Sea landmasses, then what would this mean for our understanding of ice-sheet extent in the northern hemisphere during iNHG? The onset of abundant IRD deposition in northern high-latitude oceans during MIS G6 indicates that the northern hemisphere was undoubtedly characterized by significant glaciation by 2.72 Ma. Numerical ice-sheet modelling (Bintanja and van de Wal, 2008) and evidence for enhanced North American dust deposition in the North Atlantic Ocean (which is assumed to be mainly glacially derived) from 2.72 Ma (Fig. 2C; Naafs et al., 2012) both suggest that NHG at this time included the inception of continental-ice on North America. Yet our new findings cast doubt on the assumption (Kleiven et al., 2002) that the onset of abundant IRD deposition in North Atlantic Ocean at 2.72 Ma reflects the growth of a Northeast American Ice Sheet large enough to advance any region of its grounding line onto the continental shelves adjacent to the North Atlantic Ocean.

During late Pleistocene glacials, massive volumes of icebergs carrying IRD were discharged to the subpolar North Atlantic Ocean through the Hudson Bay ice stream in North America due to the periodic collapse of the Laurentide Ice Sheet during Heinrich events (MacAyeal, 1993). For our study interval, Site 611 IRD contains only rare numbers of cream-coloured detrital limestone and does not contain feldspars with Pb-isotope compositions that are characteristic (Bond et al., 1992; Gwiazda et al., 1996a) of late Pleistocene Heinrich-events. Modelling studies (e.g. Bigg et al., 1998; Bigg and Wadley, 2001; Bigg et al., 2010) suggest that while the Hudson Bay ice stream can also produce significant numbers of icebergs during ambient Last Glacial conditions (i.e. outside of Heinrich events, during climate-driven mass-balance forced iceberg calving events), most of these icebergs pool and melt around the Labrador coast and do not reach the open North Atlantic Ocean. The south-eastern sector of the Laurentide Ice Sheet (south of ~52°N) and, in particular, the Gulf of St. Lawrence ice stream is a more probable location of any significant ambient glacial iceberg calving from North America (Bigg et al., 1998; Bigg and Wadley, 2001; Marshall and Koutnik, 2006; Watkins et al., 2007; Bigg et al., 2010) that could contribute to IRD deposition observed at Site 611 during iNHG. In this scenario, icebergs calved from this region could reach Site 611 via the North Atlantic Drift, which based of the spatial locus of maximum IRD inputs to the North Atlantic Ocean during MIS 100, was situated north of its Last Glacial position (Bailey et al., 2012).

Over 2.75–2.64 Ma, MIS G2 does not stand out in the LR04 stack as an anomalously heavy benthic $\delta^{18}O$ glacial cycle (Fig. 3A). If the distribution of feldspars at Site 611 in Pb–Pb space for MIS G2, 104 and 100 is consistent with major NHG and potentially a glacial setting in which a large Northeast American ice sheet calved significant numbers of icebergs to the subpolar North Atlantic Ocean (via, e.g. the Gulf of St. Lawrence ice stream), then either partitioning of changes in benthic $\delta^{18}O$ due to deep-sea cooling and ice-sheet expansion was highly non-linear between glacials across ~2.75–2.64 Ma and/or more of the increase in the LR04 associated with global ice-sheet expansion during MIS G6 and G4 can be attributed to the Antarctic Ice Sheet than currently appreciated (Pollard and DeConto, 2009). It is possible that any continental ice sheet that grew on northeast North America during MIS G6 and G4 remained poised just below the threshold required for it to initiate significant-rates of iceberg calving to the North Atlantic Ocean. Regardless, our findings support the notion that the maturation of continental ice on Northeast America during iNHG (taken here to occur during the first glacial for which the Pb-isotope composition of ice-rafted feldspars deposited at Site 611 is consistent with major NHG to the mid-latitudes) may have been delayed relative to the expansion of ice on Greenland and Scandinavia (Maslin et al., 1998).

The diachronous nature of ice sheet maturation in the northern hemisphere during the Pliocene may highlight the importance of regional-scale feedbacks in the climate system for the development of glacial conditions during iNHG (e.g. Ravelo et al., 2004). Enhanced poleward transport of heat and moisture via the Gulf Stream and North Atlantic Current, due to the final stages of the closure of the Central American Seaway between 3.1 and 2.6 Ma, is proposed to have provided the 'snow gun' that caused expansion of the Greenland and Scandinavian ice sheets during the late Pliocene (Sarnthein et al., 2009). Similarly, seasonal warming of surface waters in the North Pacific Ocean following the onset of Halocline stratification ~2.7 Ma is thought to have provided an upwind source of water vapour for glacial expansion on North America during MIS G6 (Haug et al., 2005). The latest state-of-the-art coupled climate-ice-sheet models indicate that ice-sheet mass balance is driven by ice-sheet ablation rather than ice accumulation (e.g. DeConto et al., 2008). The later timing of ice-sheet maturation on North America inferred in this study may, therefore, simply be attributable to the lower latitude sites of ice sheet accumulation and consequently warmer summers in these regions relative to those experienced by the circum-Arctic and Nordic Sea landmasses under the same atmospheric pCO_2 (temperature) forcing (DeConto et al., 2008).

4.5. Does the onset of the Quaternary coincide with the onset of major NHG?

MIS G6 is commonly referred to as the glacial that marks the onset of major NHG (Sigman et al., 2004; Haug et al., 2005; Swann et al., 2006; Bintanja and van de Wal, 2008; Zhang et al., 2009; Bailey et al., 2010; Etourneau et al., 2010; Ruddiman, 2010; März et al., 2013). It is legitimate, therefore, to reflect on what we really mean by this statement. Our understanding of what constitutes major NHG and when it first occurred during the Plio–Pleistocene is acutely relevant to the ongoing debate surrounding the nature and duration of the Quaternary (Head et al., 2008; Lourens, 2008; Gibbard et al., 2010). This is because the recent revision of the lower boundary of the Quaternary (and of the Pleistocene) to coincide with the Global Stratigraphic Tie Point (GSTP) for the onset of the Gelasian Stage, ~2.6 Ma, was motivated by the desire for the boundary to be drawn at a time of much greater climatic change than that purportedly associated with its former stratotype in marine strata at ~1.8 Ma (Gibbard et al., 2010). The onset of major NHG is perhaps best defined as the first time that northern hemisphere ice-sheets expanded into the mid latitudes (Head et al., 2008). If the Quaternary is defined as the 'glacial age' of the northern hemisphere (Forbes, 1846), but we accept that the history of NHG predates the Quaternary by at least ~35 Ma (Eldrett et al., 2007), then to distinguish the Quaternary from the earlier interval of the Cenozoic characterized by incipient NHG, arguably its base should coincide with evidence for the onset of major NHG.

The arguments for moving the boundary of the Quaternary to ~2.6 Ma are criticized (Lourens, 2008) on the grounds that they are less logical than moving it to the Mid–Pleistocene Transition (MPT, ~1250–700 ka), following which large amplitude 100-ka interglacial cycles of the late Pleistocene undoubtedly reflect a glacial world characterized by major NHG (Clark et al., 2006). The current choice for the lower boundary of the Quaternary is pragmatic in so far that whilst the GSTP chosen seemingly does not correspond to any particular climatic event (it coincides with the interglacial MIS 103; Ohno et al., 2012), it lies ~1 m above the Gauss–Matuyama polarity chronozone reversal within a transition of gradual glacial expansion. This choice affords an opportunity for widespread chronostratigraphic correlation between both terrestrial and marine records. Our findings highlight that the new base of the Quaternary may be closely associated in time with the first major glaciation of North America.

The magnitude of glaciation attained on orbital timescales during iNHG does not compare to that established during the large amplitude ~100-ka (inter)glacials of the late Pleistocene (Lisiecki and Raymo, 2005). Yet, convincing evidence now exists that Britain was a mid-latitude source of IRD to the North Atlantic Ocean from ~2.6 Ma (Thierens et al., 2012). Our new Pb-isotope datasets indicate that North America may have been first characterized by ice sheets that extended into the mid-latitudes as far back as MIS G2 (2.64 Ma) and most certainty was by MIS 100, 2.52 Ma (Balco and Rovey, 2010). Our suggestion that major NHG did not occur during Pliocene iNHG until 2.64 Ma is also consistent with a number of independent observations that reflect the magnitude of NHG at this time: 1) East Asian winter monsoon winds/summer monsoon precipitation strengthen/weakens dramatically from ~2.6 Ma (Sun et al., 2010; their Fig. 2), 2) meridional SST gradients in the North Pacific Ocean do not reach late Pleistocene glacial magnitudes until MIS 104, ~2.6 Ma (Brierley and Fedorov, 2010; their Fig. 1A) and, 3) terrestrial cosmogenic-nuclide burial ages of glacio-fluvial gravels in northwest North America, which mark the existence of the earliest and most extensive Cordilleran Ice Sheet (CIS), date the first CIS glacial maximum to 2.64 $^{+0.20}/_{-0.18}$ Ma (1σ; Hidy et al., 2013). Finally, recent seismic reflection studies indicate that the ice-streams that drain the Laurentide Ice Sheet in northwest Canada may not have extended onto the shelf seas that fringe the Canadian margins of northernmost Baffin Bay (Li et al., 2011) and the Beaufort Sea (Batchelor et al., 2013a,b) until ~1.6 Ma and the MPT, respectively. Thus, even if truly major NHG did not characterise glacials during the Pleistocene until after the MPT, we argue that the new base of Quaternary is closely associated the onset of the 'glacial age'.

5. Conclusions

The canonical view of Pliocene iNHG is that continental-ice sheets on Greenland, Scandinavia and North America first became marine-based and calved abundant icebergs to the Nordic Seas and subpolar North Atlantic Ocean during glacials from 2.72 Ma (during MIS G6). Our new Pb-isotope datasets, which track the provenance of ice-rafted feldspars deposited at DSDP Site 611 in the North Atlantic Ocean during iNHG, cast doubt this conclusion and suggest that prior to MIS G2 (2.64 Ma) IRD deposition in the North Atlantic Ocean was dominated by icebergs calved from Greenland and other circum-Nordic Sea landmasses. We propose that a glacial system consistent with major NHG (i.e. glaciation to mid-latitudes) first existed during the Pliocene from 2.64 Ma (from MIS G2). We further hypothesise that North America may not have been a notable source of IRD to the North Atlantic Ocean until MIS G2 (when the grounding-lines of continental ice in Northeast America extended to the adjacent North Atlantic continental shelf for the first time) and that maturation of continental ice on North America during iNHG may therefore have been delayed (by ~80 ka) relative to glacial expansion in Europe at ~2.72 Ma (Maslin et al., 1998; Foster et al., 2010). The later timing of ice-sheet maturation on North America inferred in this study is consistent with a gradual southerly expansion of northern hemisphere ice-sheets during iNHG due to top down forcing by declining pCO_2 (e.g. DeConto et al., 2008; Seki et al., 2010).

Acknowledgements

This research used samples provided by DSDP, which was sponsored by the US National Science Foundation and participating countries under management of Joint Oceanographic Institutions, Inc. We thank W. Hale and A. Wuelbers for help with sampling and J.A. Milton, D. Spanner and M. Bolshaw for laboratory assistance. We are grateful to C. Hillaire-Marcel for editorial handling and N. Fagel and an anonymous reviewer for comments and suggestions that helped to improve the manuscript. I.B. is especially grateful to S. Hemming for stimulating discussions regarding the datasets presented here and on provenance research in general. This study was supported by a Natural Environment Research Council (NERC) Research Experience Placement scheme to G.M.H. and by NERC UK IODP grants NE/F00141X/1 (I.B. and P.A.W.) and NE/H014187/1 (C.D.S and G.L.F).

Appendix A. Supplementary data

Supplementary data related to this article can be found at http://dx.doi.org/10.1016/j.quascirev.2013.06.004.

References

Backman, J., Moran, K., 2008. Introduction to special section on Cenozoic Paleoceanography of the Central Arctic Ocean. Paleoceanography 23 (1), PA1S01.

Bailey, I., Bolton, C.T., DeConto, R.M., Pollard, D., Schiebel, R., Wilson, P.A., 2010. A low threshold for North Atlantic ice-rafting from 'low-slung slippery' late Pliocene ice-sheets. Paleoceanography 25, PA1212. http://dx.doi.org/10.1029/2009PA001736.

Bailey, I., Foster, G.L., Wilson, P.A., Jovane, L., Storey, C.D., Trueman, C.N., Becker, J., 2012. The flux and provenance of ice-rafted debris in the earliest Pleistocene subpolar North Atlantic Ocean comparable to that of the Last Glacial maximum. EPSL 341–344, 222–233. http://dx.doi.org/10.1016/j.epsl.2012.05.034.

Balco, G., Rovey II, C.W., 2010. Absolute chronology for major Pleistocene advances of the Laurentide Ice Sheet. Geology 38 (9), 795–798. http://dx.doi.org/10.1130/G30946.1.

Bartoli, G., Sarnthein, M., Weinelt, M., 2006. Late Pliocene millennial-scale climate variability in the northern North Atlantic prior to and after the onset of northern hemisphere glaciation. Paleoceanography 21, PA4205,. http://dx.doi.org/10.1029/2005PA001185.

Batchelor, C.L., Dowdeswell, J.A., Pietras, J.T., 2013a. Seismic stratigraphy, sedimentary architecture and palaeo-glaciology of the Mackenzie Trough: evidence for two Quaternary ice advances and limited fan development on the western Canadian Beaufort sea margin. Quat. Sci. Revs. 65, 73–87. http://dx.doi.org/10.1016/j.quascirev.2013.01.021.

Batchelor, C.L., Dowdeswell, J.A., Pietras, J.T., 2013b. Variable history of Quaternary ice-sheet advance across the Beaufort Sea margin, Arctic Ocean. Geology 41, 131–134. http://dx.doi.org/10.1130/G33669.1.

Baumann, K.-H., Huber, R., 1999. In: Raymo, M.E., et al. (Eds.), Sea-Surface Gradients between the North Atlantic and the Norwegian Sea during the Last 3.1 m.y.: Comparison of Sites 982 and 985, Proc. ODP, Sci. Results, vol. 162. Ocean Drilling Program, College Station, TX, pp. 179–190.

Bigg, G.R., Wadley, M.R., 2001. The origin and flux of icebergs released into the Last Glacial maximum northern hemisphere oceans: the impact of ice-sheet topography. J. Quaternary Sci. 16 (6), 565–573. http://dx.doi.org/10.1002/jqs.628.

Bigg, G.R., Wadley, M.R., Stevens, D.P., Johnson, J.A., 1998. Simulations of two Last Glacial maximum states. Paleoceanography 13, 340–351.

Bigg, G.R., Levine, R.C., Clark, C.D., Greenwood, S.L., Haflidason, H., Hughes, A.L.C., Nygård, A., Sejrup, H.P., 2010. Last glacial ice-rafted debris off southwestern Europe: the role of the British–Irish Ice Sheet. J. Quaternary Sci. 25, 689–699.

Bintanja, R., van de Wal, R.S.W., 2008. North American ice-sheet dynamics and the onset of 100,000-year glacial Cycles. Nature 454. http://dx.doi.org/10.1038/nature07158.

Bolton, C.T., Wilson, P.A., Bailey, I., Friedrich, O., Beer, C.J., Becker, J., Baranwal, S., Schiebel, R., 2010. Millennial-scale climate variability in the subpolar North Atlantic Ocean during the late Pliocene. Paleoceanography 25. PA4218. http://dx.doi.org/10.1029/2010PA001951.

Bolton, C.T., Lawrence, K.T., Gibbs, S.J., Wilson, P.A., Herbert, T.D., 2011. Biotic and geochemical evidence for a global latitudinal shift in ocean biogeochemistry and export productivity during the late Pliocene. Earth Planetary Sci. Lett. 308 (1), 200–210.

Bond, G.C., Lotti, R., 1995. Iceberg discharges into the North Atlantic on millennial time scales during the last glaciation. Science 267, 1005–1010.

Bond, G.C., et al., 1992. Evidence of massive discharges of icebergs into the North Atlantic Ocean during the Last Glacial period. Nature 360, 245–249.

Brierley, C.M., Fedorov, A.V., 2010. Relative importance of meridional and zonal sea surface temperature gradients for the onset of the ice ages and Pliocene–Pleistocene climate evolution. Paleoceanography 25, PA2214. http://dx.doi.org/10.1029/2009PA001809.

Cande, S.C., Kent, D.V., 1995. Revised calibration of the geomagnetic polarity timescale for the Late Cretaceous and Cenozoic. J. Geophys. Res. 1000 (B4), 6093–6095.

Clark, P.U., Mix, A.C., 2002. Ice sheets and sea level of the Last Glacial Maximum. Quat. Sci. Revs. 21, 1–7. http://dx.doi.org/10.1016/S0277-3791(01)00118-4.

Clark, P.U., Archer, D., Pollard, D., Blum, J.D., Rial, J.A., Brovkin, V., Mix, A.C., Pisias, N.G., Roy, M., 2006. The middle Pleistocene transition: characteristics, mechanisms, and implications for long-term changes in atmospheric CO_2. Quat. Sci. Rev. 25, 3150–3184. http://dx.doi.org/10.1016/j.quascirev.2006.07.008.

Clark, P.U., Pollard, D., 1998. Origin of the middle Pleistocene transition by ice sheet erosion of regolith. Paleoceanography 13, 1–9. http://dx.doi.org/10.1029/97PA02660.

Colville, E.J., Carlson, A.E., Beard, B.L., Hatfield, R.G., Stoner, J.S., Reyes, A.V., Ullman, D.J., 2011. Sr–Nd–Pb isotope evidence for ice-sheet presence on southern Greenland during the Last Interglacial. Science 333 (6042), 620–623.

DeConto, R.M., Pollard, D., Wilson, P.A., Palike, H., Lear, C.H., Pagani, M., 2008. Thresholds for Cenozoic bipolar glaciation. Nature 455, 652–656. http://dx.doi.org/10.1038/nature07337.

De'Ath, R., Siegert, M.J., Bigg, G.R., Wadley, M.R., 2006. Modelling iceberg trajectories, sedimentation rates and meltwater input to the ocean from the Eurasian ice sheet at the Last Glacial maximum. Palaeogeog. Palaeoclim. Palaeoecol. 236, 135–150.

Einarsson, T., Albertsson, K.J., 1988. The glacial history of Iceland during the past three million years. In: Shackleton, N.J., et al. (Eds.), The Past Three Million Years: Evolution of Climatic Variability in the North Atlantic region. The Royal Society, London, pp. 227–234.

Eldrett, J.S., Harding, I.C., Wilson, P.A., Butler, E., Roberts, A.P., 2007. Continental ice in Greenland during the Eocene and Oligocene. Nature 446 (7132), 176–179. http://dx.doi.org/10.1038/nature05591.

Etourneau, J., Schneider, R., Blanz, T., Martinez, P., 2010. Intensification of the Walker and Hadley atmospheric circulations during the Pliocene–Pleistocene climate transition. Earth Planetary Sci. Lett. 297 (1), 103–110.

Fagel, N., Innocent, C., Gariépy, C., Hillaire-Marcel, C., 2002. Sources of Labrador Sea sediments since the Last Glacial Maximum inferred from Nd–Pb isotopes. Geochim. Cosmochim. Acta 66, 2569–2581.

Farmer, G.L., Barberb, D., Andrews, J., 2003. Provenance of Late Quaternary ice-proximal sediments in the North Atlantic: Nd, Sr and Pb isotopic evidence. Earth Planetary Sci. Lett. 209, 227–243.

Forbes, E., 1846. On the Connection Between the Distribution of the Existing Fauna and Flora of the British Isles, and the Geological Changes Which Have Affected Their Area, Especially During the Epoch of the Northern Drift: Great Britain Geological Survey Memoir, vol. 1, pp. 336–342.

Foster, G.L., Lunt, D.J., Parrish, R.R., 2010. Mountain uplift and the glaciation of North America – a sensitivity study. Clim. Past 6, 707–717. http://dx.doi.org/10.5194/cp-6-707-2010.

Fronval, T., Jansen, E., 1996. Late Neogene Paleoclimates and Paleoceanography in the Iceland-Norwegian Sea. In: Thiede, J., Myhre, A.M., Futh, J.V., Johnson, G.L., Ruddiman, W. (Eds.), Proc. ODP, Sci Repts., 151. College Station, TX, 455–468.

Gao, C., McAndrews, J.H., Wang, X., Menzies, J., Turton, C.L., Wood, B.D., Pei, J., Kodors, C., 2012. Glaciation of North America in the James Bay Lowland, Canada, 3.5 Ma. Geology 40 (11), 975–978. http://dx.doi.org/10.1130/G33092.1.

Geirsdóttir, Á., Eiríksson, J., 1994. Growth of an intermittent Ice Sheet in Iceland during the Late Pliocene and Early Pleistocene. Quat. Res. 42, 115–130.

Geissler, W.H., Jokat, W., 2004. A geophysical study of the northern Svalbard continental margin. Geophys. J. Int. 158, 50–66.

Gibbard, P., Head, M.J., Walker, M.J.C., The Subcommission on Quaternary Stratigraphy, 2010. Formal ratification of the Quaternary system/period and the Pleistocene Series/Epoch with a base at 2.58 Ma. J. Quaternary Sci. 25, 96–102.

Gwiazda, R.H., Hemming, S.R., Broecker, W.S., 1996a. Tracking the sources of icebergs with lead isotopes: the provenance of ice-rafted debris in Heinrich layer 2. Paleoceanography 11 (1), 77–93.

Gwiazda, R.H., Hemming, S.R., Broecker, W.S., 1996b. Provenance of icebergs during Heinrich event 3 and the contrast to their sources during other Heinrich episodes. Paleoceanography 11 (4), 371–378.

Haug, G.H., Tiedemann, R., 1998. Effect of the formation of the isthmus of Panama on Atlantic Ocean thermohaline circulation. Nature 393, 673–676.

Haug, G.H., Ganopolski, A., Sigman, D.M., Rosell-Mele, A., Swann, G.E.A., Tiedemann, R., Jaccard, S.L., Bollmann, J., Maslin, M.A., Leng, M.J., Eglinton, G., 2005. North Pacific seasonality and the glaciation of North America 2.7 million years ago. Nature 433, 821–825.

Hayashi, T., Ohno, M., Acton, G., Guyodo, Y., Evans, H.F., Kanamatsu, T., Komatsu, F., Murakami, F., 2010. Millennial-scale iceberg surges after intensification of northern hemisphere glaciation. Geochem. Geophys. Geosyst. 11, Q09Z20. http://dx.doi.org/10.1029/2010GC003132.

Head, M.J., Gibbard, P., Salvador, A., 2008. The Quaternary: its character and definition. Episodes 31 (2), 234.

Henrich, R., Baumann, K.H., 1994. Evolution of the Norwegian Current and the Scandinavian Ice Sheets during the past 2.6 m.y.: evidence from ODP Leg 104 biogenic carbonate and terrigenous records. Palaeogeography, Palaeoclimatology, Palaeoecology 108, 75–94.

Hemming, S.R., 2004. Heinrich events: massive late Pleistocene detritus layers of the North Atlantic and their global climate imprint. Rev. Geophys. 42, RG1005. http://dx.doi.org/10.1029/2003RG000128.

Henriksen, N., 2008. Geological History of Greenland. Geological Survey of Denmark and Greenland, Copenhagen, p. 270.

Hidy, A.J., Gosse, J.C., Froese, D.G., Bond, J.D., Rood, D.H., 2013. A latest Pliocene age for the earliest and most extensive Cordilleran Ice Sheet in northwestern Canada. Quat. Sci. Revs. 61, 77–84. http://dx.doi.org/10.1016/j.quascirev.2012.11.009.

Jansen, E., Sjøholm, J., 1991. Reconstruction of glaciation over the past 6 Myr from ice-borne deposits in the Norwegian Sea. Nature 349, 600–603.

Jansen, E., Sjøholm, J., Bleil, U., Erichsen, J.A., 1990. Neogene and Pleistocene glaciations in the northern hemisphere and late Miocene–Pliocene global ice volume fluctuations: evidence from the Norwegian Sea. In: Bleil, U., Thiede, J. (Eds.), Geological History of the Polar Oceans: Arctic Versus Antarctic. Kluwer Academic, Dordrecht, pp. 677–705.

Jansen, E., Fronval, T., Rack, F., Channell, J.E.T., 2000. Pliocene–Pleistocene ice rafting history and cyclicity in the Nordic Seas during the last 3.5 Myr. Paleoceanography 15 (6), 709–721.

Joyce, J.E., Tjalsma, L.R.C., Prutzman, J.M., 1993. North American glacial meltwater history for the past 2.3My: oxygen isotope evidence from the Gulf of Mexico. Geology 21, 483–486.

Kleiven, H.F., Jansen, E., Fronval, T., Smith, T.M., 2002. Intensification of northern hemisphere glaciations in the circum Atlantic region (3.5–2.4 Ma) – ice-rafted detritus evidence. Palaeogeog. Palaeoclim. Palaeoecol. 184, 213–223.

Knies, J., Matthiessen, J., Vogt, C., Laberg, J.S., Hjelstuen, B.O., Smelror, M., Larsen, E., Andreassen, K., Eidvin, T., Vorren, T.O., 2009. The Plio-Pleistocene glaciation of the Barents Sea-Svalbard region: a new model based on revised chro-nostratigraphy. Quat. Sci. Rev. 28, 812–829.

Krissek, L.A., 1989. Late Cenozoic records of ice-rafting at ODP sites 642, 643 and 644, Norwegian Sea: onset, chronology, and characteristics of glacial/interglacial fluctuations. In: Eldholm, O., Thiede, J., Taylor, E. (Eds.), Proceedings of the Ocean Drilling Project. Scientific Results, vol. 104, pp. 61–69.

Li, G., Piper, D.J.W., Campbell, D.C., 2011. The Quaternary lancaster sound trough-mouth fan, NW Baffin Bay. J. Quaternary Sci. 26 (5), 511–522.

Lisiecki, L.E., Raymo, M.E., 2005. A Pliocene–Pleistocene stack of 57 globally distributed benthic delta-^{18}O records. Paleoceanography 20, PA1003. http://dx.doi.org/10.1029/2005PA001164.

Lourens, L.J., 2008. On the Neogene–Quaternary debate. Episodes 31 (2), 239.

Lunt, D.J., Foster, G.L., Haywood, A.M., Stone, E.J., 2008. Late Pliocene Greenland glaciation controlled by a decline in atmospheric CO_2 levels. Nature 454, 1102–1106. http://dx.doi.org/10.1038/nature07223. doi:10.1029/2005PA001247.

MacAyeal, D.R., 1993. A low-order model of the Heinrich event cycle. Paleoceanography 8, 767–773.

Maccali, J., Hillaire-Marcel, C., Carignan, J., Reisberg, L.C., 2012. Pb isotopes and geochemical monitoring of Arctic sedimentary supplies and water mass export through Fram Strait since the Last Glacial Maximum. Paleoceanography 27, PA1201. http://dx.doi.org/10.1029/2011PA002152.

Marshall, S.J., Koutnik, M.R., 2006. Ice sheet action versus reaction: distinguishing between Heinrich events and Dansgaard-Oeschger cycles in the North Atlantic. Paleoceanography 21, PA2021. http://dx.doi.org/10.1029/2005PA001247.

März, C., Schnetger, B., Brumsack, H.-J., 2013. Nutrient leakage from the North Pacific to the Bering Sea (IODP Site U1341) following the onset of Northern Hemispheric glaciation? Paleoceanography 28 (1), 68–78, http://dx.doi.org/10.1002/palo.20011.

Maslin, M.A., Li, X.S., Loutre, M.-F., Berger, A., 1998. The contribution of orbital forcing to the progressive intensification of northern hemisphere glaciation. Quat. Sci. Revs. 17, 411–426.

Miller, K.G., Wright, J.D., Browning, J.V., Kulpecz, A.A., Kominz, M.A., Naish, T.R., Cramer, B.S., Rosenthal, Y., Peltier, R.W., Sosdian, S., 2012. The high tide of the warm Pliocene: implications of global sea level for Antarctic deglaciation. Geology 40, 407–410.

Mudelsee, M., Raymo, M.E., 2005. Slow dynamics of the northern hemisphere glaciation. Paleoceanography 20, PA4022. http://dx.doi.org/10.1029/2005PA001153.

Naafs, B.D.A., Hefter, J., Acton, G., Haug, G.H., Martínez-Garcia, A., Pancost, R., Ruediger, S.R., 2012. Strengthening of North American dust sources during the late Pliocene (2.7 Ma). EPSL 317–318, 8–19. http://dx.doi.org/10.1016/j.epsl.2011.11.026.

Naish, T., 1997. Constraints on the amplitude of late Pliocene eustatic sea level fluctuations: new evidence from the New Zealand shallow marine sediment record. Geology 25 (12), 1139–1142. http://dx.doi.org/10.1130/0091-(1997)025 < 1139:COTAOL > 2.3.CO;2.

Ohno, M., Hayashi, T., Komatsu, F., Murakami, F., Zhao, M., Guyodo, Y., Kanamatsu, T., 2012. A detailed paleomagnetic record between 2.1 and 2.75 Ma at IODP Site U1314 in the North Atlantic: geomagnetic excursions and the Gauss–Matuyama transition. Geochem. Geophys. Geosyst. 13 (1), Q12Z39. http://dx.doi.org/10.1029/2012GC004080.

Pollard, D., DeConto, R.M., 2009. Modeling West Antarctic ice sheet growth and collapse. Nature 458, 329–332. http://dx.doi.org/10.1038/nature07809.

Peck, V.L., Hall, I.R., Zahn, R., Grousset, F., Hemming, S.R., Scourse, J.D., 2007. The relationship of Heinrich events and their European precursors over the past 60 ka BP: multi-proxy ice-rafted debris provenance study in the North East Atlantic. Quat. Sci. Rev. 26. http://dx.doi.org/10.1016/j.quascirev.2006.12.002.

Prell, W.L., 1984. Covariance patterns of foraminiferal d18O: an evaluation of Pliocene ice volume changes near 3.2 million years ago. Science 226, 692–694. http://dx.doi.org/10.1126/science.226.4675.692.

Ravelo, A.C., Andreasen, D.H., Lyle, M., Lyle, A.O., Wara, M.W., 2004. Regional climate shifts caused by gradual global cooling in the Pliocene epoch. Nature 429. http://dx.doi.org/10.1038/nature02567.

Raymo, M.E., Ruddiman, W.F., Backman, J., Clement, B.M., Martinson, D.G., 1989. Late Pliocene variation in northern hemisphere ice sheets and North Atlantic deep circulation. Paleoceanography 4, 413–446.

Raymo, M.E., Hodell, D., Jansen, E., 1992. Response of deep ocean circulation to the initiation of northern hemisphere glaciation (3–2 M.Y.). Paleoceanography 7, 645–672.

Ruddiman, W.F., 1977. Late Quaternary deposition of ice-rafted sand in the subpolar North Atlantic (lat 40–65 N). Geol. Soc. Am. Bull. 88, 1813–1827. http://dx.doi.org/10.1130/0016-606(1977)88 < 1813:LQDOIS > 2.0.CO;2.

Ruddiman, W.F., 2010. A Paleoclimatic enigma? Science 328 (5980), 838–839.

Ruddiman, W.F., Raymo, M.E., 1988. Northern hemisphere climate regimes during the past 3 Ma: possible tectonic connections. Philos. Trans. Royal Soc. Lond. B 318, 411–430.

Sarkar, S., Berndt, C., Chabert, A., Masson, D.G., Minshull, T.A., Westbrook, G.K., 2011. Switching of a paleo-ice stream in northwest Svalbard. Quat. Sci. Rev. 30 (13–14), 1710–1725. http://dx.doi.org/10.1016/j.quascirev.2011.03.013.

Sarnthein, M., Bartoli, G., Prange, M., Schmittner, A., Schneider, B., Weinelt, M., Andersen, N., Garbe-Schönberg, D., 2009. Mid-Pliocene shifts in ocean overturning circulation and the onset of Quaternary-style climates. Clim. Past 5, 269–283. www.clim-past.net/5/269/2009/.

Seki, O., Foster, G.L., Schmidt, D.N., Mackensen, A., Kawamura, K., Pancost, R.D., 2010. Alkenone and boron-based Pliocene pCO_2 records. Earth Planet. Sci. Lett. 292, 201–211.

Shackleton, N.J., Hall, M.A., 1984. Oxygen and carbon isotope stratigraphy of deep sea drilling Project Hole 552A: Plio–Pleistocene glacial history. Init. Repts. DSDP 74, 599–609.

Shackleton, N.J., et al., 1984. Oxygen isotope calibration of the onset of ice-rafting and history of glaciation in the North Atlantic region. Nature 307, 620–623.

Shipboard Scientific Party, 1987. Site 611. In: Ruddiman, W.E., Kidd, R.B., Thomas, E., et al. (Eds.), Initital Reports DSDP, vol. 94. In: http://dx.doi.org/10.2973/dsdp.proc.94.107.1987.

Shipboard Scientific Party, 1996. Site 982. Proc. Ocean Drill. Program Initial Rep. 162, 91–138. http://dx.doi.org/10.2973/odp.proc.ir.162.104.1996.

Sigman, D.M., Jaccard, S., Haug, G.H., 2004. Polar ocean stratification in a cold climate. Nature 428, 59–63.

Stoker, M.S., Leslie, A.B., Scott, W.D., Briden, J.C., Hine, N.M., Harland, R., Wilkinson, I.P., Evans, D., Ardus, D.A., 1994. A record of late Cenozoic stratigraphy, sedimentation and climate change from the Hebrides slope, NE Atlantic Ocean. J. Geol. Soc. Lond 151, 235–249.

Sun, Y., An, Z., Clemens, S.C., Bloemendal, J., Vandenberghe, J., 2010. Seven million years of wind and precipitation variability on the Chinese Loess Plateau. EPSL 297, 525–535.

Swann, G.E.A., Maslin, M.A.., Leng, M.J., Sloane, H.J., Haug, G.H., 2006. Diatom $\delta^{18}O$ evidence for the development of the modern halocline system in the subarctic northwest Pacific at the onset of major northern hemisphere glaciation. Paleoceanography 21, PA1009. http://dx.doi.org/10.1029/2005PA001147.

Thierens, M., Pirlet, H., Colin, C., Latruwe, K., Vanhaecke, F., Lee, J.R., Stuut, J.-B., Titschack, J., Huvenne, V.A.I., Dorschel, B., Wheeler, A.J., Henriet, J.-P., 2012. Ice-rafting from the British–Irish ice sheet since the earliest Pleistocene (2.6 million years ago): implications for long-term mid-latitudinal ice-sheet growth in the North Atlantic region. Quat. Sci. Revs. 44, 229–240. http://dx.doi.org/10.1016/j.quascirev.2010.12.020.

Watkins, S.J., Maher, B.A., Bigg, G.R., 2007. Ocean circulation at the Last Glacial Maximum: a combined modeling and magnetic proxy-based study. Paleoceanography 22, PA2204. http://dx.doi.org/10.1029/2006PA001281.

Zhang, Y.G., Ji, J., Balsam, W., Liu, L., Chen, J., 2009. Mid-Pliocene Asian monsoon intensification and the onset of northern hemisphere glaciation. Geology 37 (7), 599–602.